Spatio-temporal sequence of cross-regulatory events in root meristem growth

Emanuele Scacchi[a], Paula Salinas[a], Bojan Gujas[a], Luca Santuari[a], Naden Krogan[b], Laura Ragni[a], Thomas Berleth[b], and Christian S. Hardtke[a,1]

[a]Department of Plant Molecular Biology, University of Lausanne, CH-1015 Lausanne, Switzerland; and [b]Department of Cell and Systems Biology, University of Toronto, Toronto, ON, Canada M5S 3B2

Edited by Philip Benfey, Duke University, Durham, NC, and approved November 22, 2010 (received for review September 30, 2010)

A central question in developmental biology is how multicellular organisms coordinate cell division and differentiation to determine organ size. In Arabidopsis roots, this balance is controlled by cytokinin-induced expression of *SHORT HYPOCOTYL 2* (*SHY2*) in the so-called transition zone of the meristem, where SHY2 negatively regulates auxin response factors (ARFs) by protein–protein interaction. The resulting down-regulation of *PIN-FORMED* (*PIN*) auxin efflux carriers is considered the key event in promoting differentiation of meristematic cells. Here we show that this regulation involves additional, intermediary factors and is spatio-temporally constrained. We found that the described cytokinin–auxin crosstalk antagonizes *BREVIS RADIX* (*BRX*) activity in the developing protophloem. *BRX* is an auxin-responsive target of the prototypical ARF MONOPTEROS (MP), a key promoter of vascular development, and transiently enhances *PIN3* expression to promote meristem growth in young roots. At later stages, cytokinin induction of *SHY2* in the vascular transition zone restricts *BRX* expression to down-regulate *PIN3* and thus limit meristem growth. Interestingly, proper *SHY2* expression requires *BRX*, which could reflect feedback on the auxin responsiveness of *SHY2* because BRX protein can directly interact with MP, likely acting as a cofactor. Thus, cross-regulatory antagonism between *BRX* and *SHY2* could determine ARF activity in the protophloem. Our data suggest a model in which the regulatory interactions favor *BRX* expression in the early proximal meristem and *SHY2* prevails because of supplementary cytokinin induction in the later distal meristem. The complex equilibrium of this regulatory module might represent a universal switch in the transition toward differentiation in various developmental contexts.

In multicellular organisms, coordinated balance between cell division and differentiation determines organ size. In *Arabidopsis thaliana* (Arabidopsis), this can be easily observed along a proximo-distal sequence in the root meristem, where stem-cell daughters divide repeatedly before eventually starting to elongate and differentiate (1). Two principal meristematic regions can be distinguished: a proximal (i.e., closer to the root tip) division zone and a distal elongation zone. These are connected by a transition zone, which stands out in the developing protophloem as a series of partially elongated cells that no longer divide but also transiently cease to elongate (Fig. 1*A*). The zones represent a useful formalism for describing the underlying spatio-temporal gradient of individual cell ontogeny, where the temporal component is age and the spatial component is distance from the stem-cell niche (Fig. 1*B*). Cell ontogeny responds to systemic cues, most notably an auxin gradient across the root meristem (4) that is established by a self-organizing system of transcellular polar auxin transport (PAT) (5, 6). PAT direction and amplitude depend on the polarity and amount of PIN proteins, feedback-regulated transmembrane auxin efflux carriers whose activity can be modulated by endogenous signals to trigger developmental decisions (7).

A recent example is the down-regulation of *PIN* expression in the transition zone, which is thought to be the key event in promoting cell differentiation and thus in determining meristem size and consequently root growth rate (8–10). This phenomenon is triggered by cytokinin-induced expression of SHY2/IAA3 (SHY2 in the following), an AUXIN/INDOLE-ACETIC ACID (AUX/IAA)-type protein that suppresses the activity of auxin response factors (ARFs) through protein–protein interaction and thus suppresses expression of auxin-responsive genes (11), which include *PIN* genes. Dominant *shy2* (*shy2-D*) mutants that encode stabilized SHY2 protein therefore display premature cell differentiation and consequently smaller meristem size (9). Another mutant with reduced root meristem size is *brx*, which was initially isolated as a quantitative trait locus through the natural variation approach and encodes a putative transcriptional coregulator (12, 13). Subsequent analyses revealed that *BRX* is also needed for optimal growth in the radial dimension of the root as well as optimal shoot growth (14, 15). *BRX* is expressed in the vasculature and is rate-limiting for transcriptional auxin action (16), possibly by impinging on the biosynthesis of brassinosteroids, which are thought to synergistically promote auxin signaling or PAT (17–20). Moreover, *BRX* activity is controlled by auxin at both the transcriptional and posttranslational level. *BRX* expression is positively feedback-regulated by auxin signaling (16), and auxin also promotes translocation of BRX protein from the plasma membrane into the nucleus, where it is thought to regulate interacting transcription factors (21). Starting from the phenotypic congruency between *brx* and *shy2-D* mutants, we show here that the two genes act antagonistically through cross-regulatory interactions to determine meristem growth during early root development.

Results and Discussion

The *brx* loss-of-function mutants display reduced root meristem size, a phenotype that manifests strongly only toward the end of meristem growth (13, 22) (Fig. S1*A*) at 5–6 d after germination (dag), thereby phenocopying *shy2-D* (9). In root meristems of young seedlings, *BRX* is expressed in the developing protophloem up to the elongation zone (Fig. 1*C*), with distal expression fading as plants grow older (Fig. 1*D*). A marker of phloem identity, *ALTERED PHLOEM DEVELOPMENT* (*APL*) (23), is still expressed in *brx* mutants, suggesting that phloem fate is correctly specified (Fig. 1*E*). However, both *APL* expression and protophloem-specific cell-wall staining (2) revealed asynchronous progression of distal protophloem development (Fig. 1 *E* and *F*) and premature recruitment of cells into the elongation zone in *brx* mutants (Fig. 1*G*), suggesting a cell-autonomous role of *BRX* in the timing of protophloem differentiation.

Author contributions: E.S., P.S., B.G., T.B., and C.S.H. designed research; E.S., P.S., B.G., N.K., and L.R. performed research; E.S., P.S., B.G., L.S., N.K., L.R., T.B., and C.S.H. analyzed data; and E.S. and C.S.H. wrote the paper.

The authors declare no conflict of interest.

This article is a PNAS Direct Submission.

[1]To whom correspondence should be addressed. E-mail: christian.hardtke@unil.ch.

This article contains supporting information online at www.pnas.org/lookup/suppl/doi:10.1073/pnas.1014716108/-/DCSupplemental.

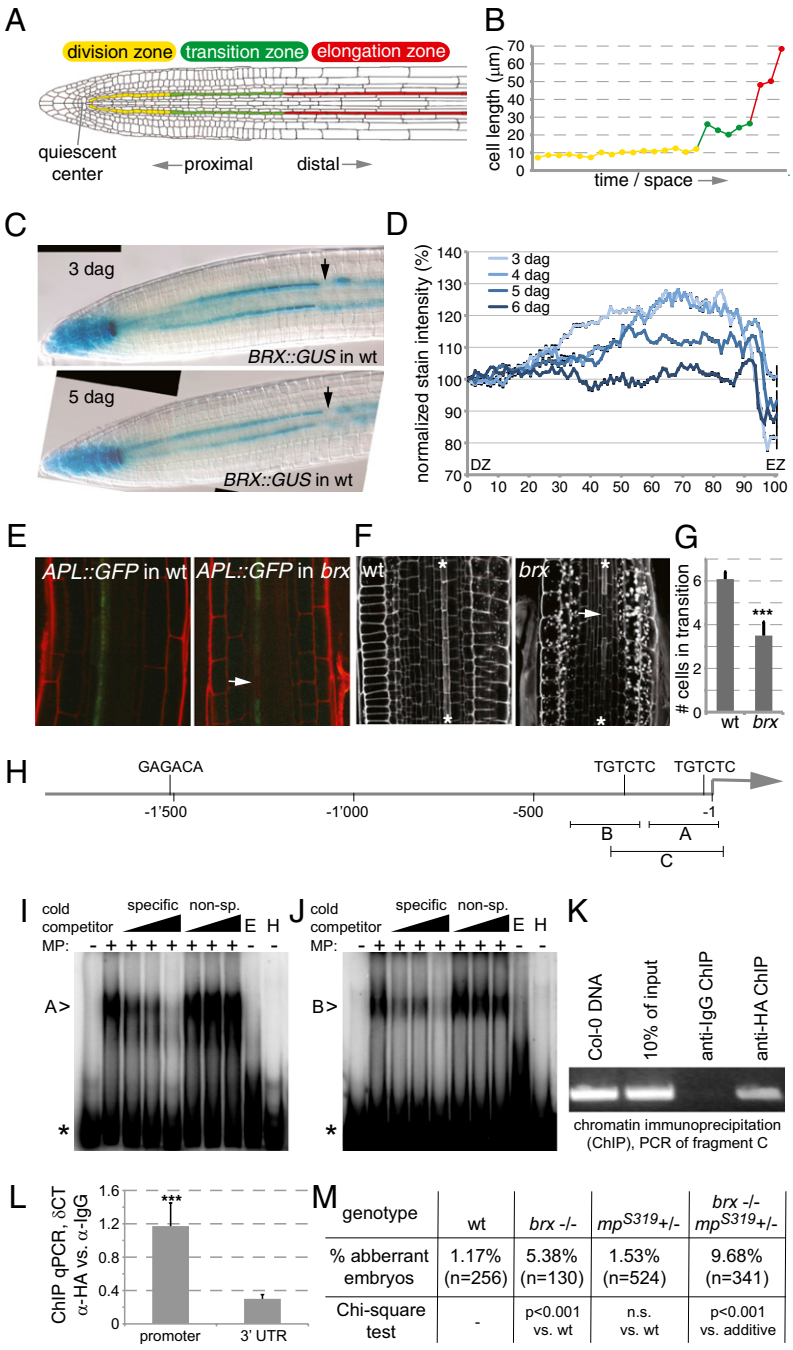

Fig. 1. *BRX* is an MP target gene. (*A*) Schematic overview of the Arabidopsis root meristem with protophloem highlighted. (*B*) Progression of cell elongation in the protophloem. (*C*) *BRX::GUS* reporter gene expression in columella, stem-cell niche, and protophloem of wild-type (wt) root meristems at 3 and 5 d dag. Arrowheads indicate the first protophloem elongation zone cells. (*D*) Quantitative protophloem expression profiles of *BRX::GUS* across the division zone (DZ) and transition zone up to the elongation zone (EZ). $n = 18$ for 3, 4, and 5 dag; $n = 10$ for 6 dag. (*E*) Expression of *APL::GFP* in wt and *brx* at 5 dag. Arrowhead indicates a gap in expression. (*F*) Protophloem-specific cell-wall staining (2) at 5 dag. Arrowhead indicates a staining gap in *brx*. (*G*) Number of cells in the protophloem transition zone in wt and *brx* at 5 dag. (*H*) Schematic view of *BRX* promoter with ARF-binding sites indicated. (*I* and *J*) Electrophoretic mobility shift assay of *BRX* promoter fragments (*H*) with a recombinant His-tagged fragment of MP protein (amino acids 1–432) containing the DNA-binding domain. E: no protein added; H: an unrelated His-tagged protein added; asterisks: free probe. (*K* and *L*) Replicate ChIPs of *BRX* promoter with transgenic HA-tagged MP protein (3), analyzed by semiquantitative PCR (*K*) or qPCR (*L*). (*M*) Frequency of aberrant embryos in wt, *brx*, mp^{S319}, and *brx* mutants segregating 1/4 *brx* mp^{S319} double mutants. Error bars in *D*, *G*, and *L* indicate SE. ***$P < 0.001$.

BRX is among the earliest markers of protophloem development from embryogenesis onward (16, 24), similar to *MP*, a master regulator of vascular development and root formation (25, 26). Auxin responsiveness and prototypical ARF-binding sites in the *BRX* promoter (16) (Fig. 1*H*), as well as similar expression patterns of *BRX* and *MP* already manifested during embryogenesis (21, 25), suggested that *BRX* might be an *MP* target gene. We confirmed this notion by in vitro gel-shift experiments with the *BRX* promoter using a recombinant MP protein fragment that encompassed the DNA-binding domain, as well as by chromatin immunoprecipita-

tion with a tagged, full-length *MP* transgene (3) (Fig. 1 *I–L*). Supporting genetic interaction was difficult to establish because of the essential nature of *MP* for root formation. However, *brx* mutants display a low penetrance, *mp*-like embryo phenotype, which was synergistically enhanced in plants segregating double mutants with the weak mp^{S319} allele (3) (Fig. 1*M*), suggesting that *MP* regulation of *BRX* is biologically relevant.

Interestingly, SHY2 is able to negatively regulate the transcription activation potential of MP and redundantly acting ARFs (11), suggesting that it might negatively regulate *BRX*. Reporter gene analyses revealed that detectable *SHY2* and *BRX* expression is indeed largely mutually exclusive in root meristems (Fig. 2 *A–C*). *SHY2* is only very weakly expressed in the developing protophloem (27) and generally not detectable by reporter gene assays. However, expression can be detected in the more distal protophloem and eventually throughout the vascular cylinder in the elongation zone (Fig. S1*B*). Overlap of detectable *BRX* and *SHY2* expression is observed in only a few cells, mostly in the transition zone of the protophloem. Moreover, whereas distal *BRX* expression decreases progressively as roots get older (Fig. 1*C*), distal *SHY2* expression increases simultaneously (Fig. 2*B*) (9). Further, *BRX* expression is deregulated in *shy2-31* loss-of-function mutants and invades the *SHY2* expression domain (Fig. 2*C*; Fig. S1*C*). This is, for example, evident in the protoxylem, where *SHY2* expression can be detected from early on, whereas *BRX* expression is normally barely, if at all, detectable (Fig. S1*B*). These findings suggest not only that *BRX* expression is down-regulated by *SHY2*, but also that *BRX* expression should be cytokinin-responsive. Indeed, cytokinin application results in the down-regulation of *BRX* in distal protophloem (Fig. 2*D*) at the transition zone, where *SHY2* expression is simultaneously induced (9). Consistent with these findings, root growth and meristem size in *brx* mutants is no longer cytokinin-responsive (Fig. 2 *E* and *F*). The combined experimental evidence thus supports the idea that the described cytokinin–auxin crosstalk regulates meristem size through suppression of *BRX* expression during later stages of protophloem development.

Cytokinin-induced *SHY2* activity in the transition zone down-regulates *PIN* expression, which is thought to be a direct effect of ARF inhibition (9, 10). Among those *PIN* genes, *PIN3* has been reported to be under-expressed in *brx* roots (16), a result that we corroborated by quantitative real-time PCR (qPCR) (Fig. S1*D*). This result was also confirmed by examination of a *PIN3::PIN3:GFP* transgene (7) in young *brx* meristems at 3 dag (Fig. 3 *A* and *B*), when *brx* and wild-type meristems are still of similar size (Fig. S1*A*). However, reduced *PIN3* expression in *brx* was no longer observed by both methods from 5 dag onward (Fig. 3 *C* and *D*; Fig. S1*D*). To investigate this phenomenon in situ, we measured PIN3-GFP intensity along the developing protophloem at 3 and 5 dag (Fig. 3 *E* and *F*). We found that at 3 dag PIN3 levels were lowest in early stem-cell daughters and gradually increased up to and across the transition zone before falling back to lower levels. At 5 dag, this bell-shaped profile had flattened, resembling the PIN3 expression pattern observed in *brx* mutants from early on. Interestingly, the wild-type peak of PIN3 abundance in the early meristem coincided with a gradient of decreasing BRX-GFP plasma membrane localization, which culminated in the transition zone and suggests that BRX enters the nucleus as protophloem development progresses (Fig. 3*G*; Fig. S1 *E–G*). Notably, the loss of *PIN3* expression in *brx* was not cross-complemented by enhanced expression of other *PIN* genes (28) (Fig. 3 *H* and *I*; Fig. S1*H*). Moreover, qPCR quantification of all meristematic *PIN* genes suggests that *PIN3* is the dominant *PIN* gene in early meristem development (Fig. S1*H*). Finally, in *brx* roots, neither *PIN3* expression levels nor the *PIN3* expression profile could be altered by cytokinin application any longer (Fig. 3 *J* and *K*). Collectively, these observations suggest that *BRX* mediates the cytokinin effect and is necessary to enhance *PIN3* expression during early root development to promote meristem growth and determine final meristem size. This finding also matches with the previous observation that pharmacological inhibition of PAT in wild-type root tips mimics the *brx* root meristem phenotype (21).

Interestingly, PIN3 levels are strongly reduced throughout the provascular and ground tissues in young *brx* meristems (Fig. 3*B*),

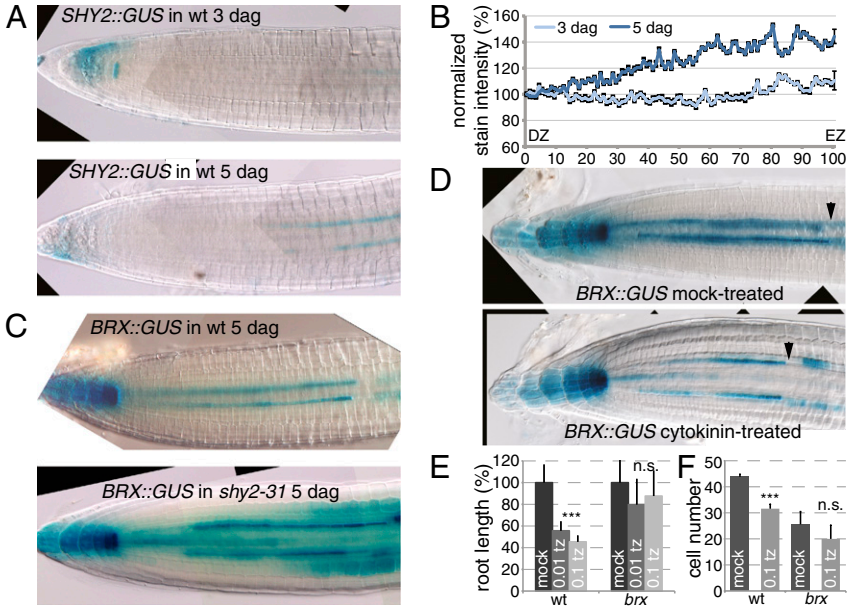

Fig. 2. *BRX* control by *SHY2*. (*A* and *B*) Expression pattern of *SHY2::GUS* reporter gene in wild-type (wt) roots (*A*) and quantitative expression profiles (*B*). $n = 6$ for 3 dag; $n = 4$ for 6 dag. (*C*) *BRX::GUS* reporter gene expression in wt roots and enhanced and ectopic expression of *BRX::GUS* in *shy2-31* loss-of-function mutants. Note enhanced *BRX* expression in the protoxylem strip at the center of the *shy2-31* root. (*D*) Repression and proximal shift (arrowheads) of *BRX::GUS* expression after 6 h cytokinin [5 μM transzeatin (tz)] treatment. (*E* and *F*) Cytokinin insensitivity of *brx* root growth (*E*) and meristem size (meristematic cortex cell number) (*F*). Error bars in *B*, *E*, and *F* indicate SE. ***$P < 0.001$; n.s.: not significant.

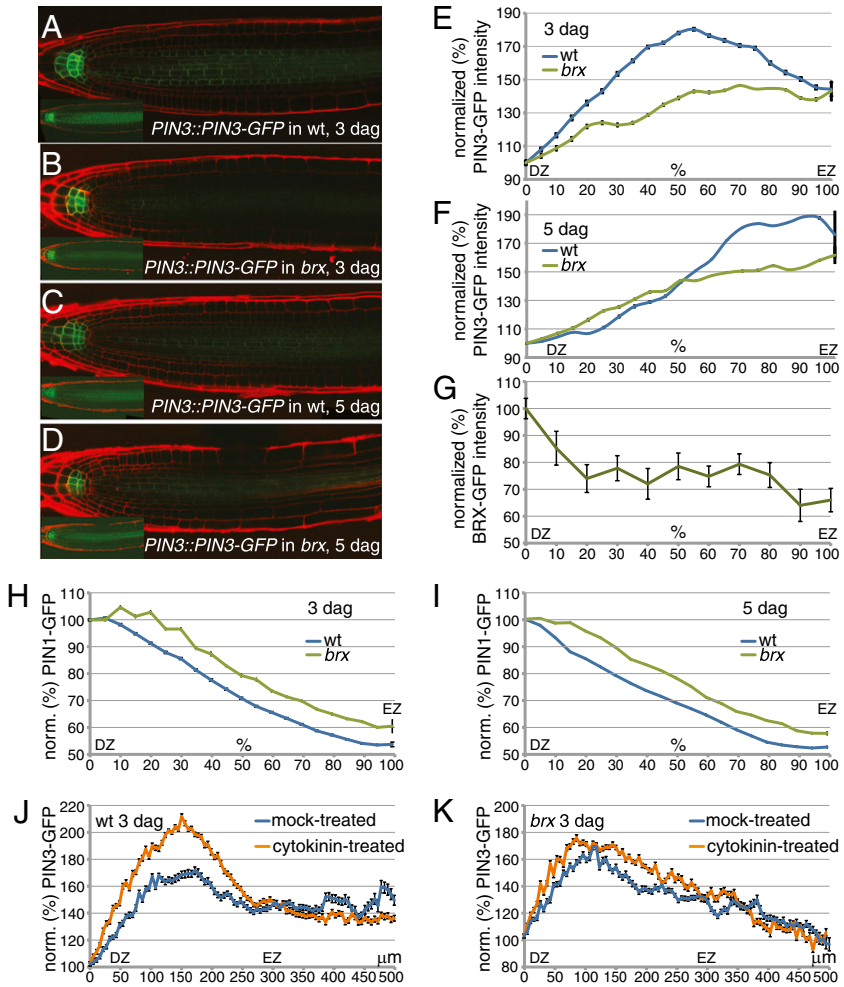

Fig. 3. Enhancement of *PIN3* expression by *BRX* in early meristems. (*A–D*) Expression of *PIN3::PIN3-GFP* transgene in wild-type (wt) and *brx* background at 3 and 5 dag. *Insets* show images with green channel digitally enhanced. (*E* and *F*) Quantitative expression profiles of *PIN3::PIN3-GFP* across the two protophloem poles in wt and *brx* at 3 and 5 dag. *n* (wt) = 18 and *n* (*brx*) = 8 for 3 dag; *n* (wt) = 8 and *n* (*brx*) = 12 for 5 dag. (*G*) Relative quantitative plasma membrane abundance of BRX-GFP fusion protein in the protophloem. *n* = 13. (*H* and *I*) Quantitative expression profiles of *PIN1::PIN1-GFP* across the two protophloem poles in wt and *brx* at 3 and 5 dag. *n* (wt) = 20 and *n* (*brx*) = 10 for 3 dag; *n* (wt) = 16 and *n* (*brx*) = 30 for 5 dag. (*J*) Expression profile of *PIN3::PIN3-GFP* along the root meristem at 3 dag after mock or cytokinin (6 h of 5 µM transzeatin) treatment. *n* = 16 for mock and *n* = 20 for cytokinin treatment. (*K*) Same as in *J* but for *brx*. *n* = 14 for mock and cytokinin treatment. Error bars in *E–K* indicate SE. DZ: beginning of the division zone; EZ: position of first elongation zone cell; Note that for expression profile comparisons starting points have been set to 100%; i.e., curves do not indicate absolute expression levels. For intergenotype comparisons, meristem size was scaled to a percentage.

although *BRX* expression is restricted to the protophloem. This suggests a non–cell-autonomous, systemic effect of *BRX* action, although *BRX* mRNA or protein does not appear to move (16, 21). Therefore, the systemic effect could reflect either a self-regulatory feature of PAT (5, 6) or an additional positive effect of *BRX* on the biosynthesis of brassinosteroids (14, 16), which have been described to systemically enhance PAT (17, 19, 29). The observation that meristem growth is reduced by the application of the brassinosteroid biosynthesis inhibitor brassinazole in wild type, but not in *brx* (Fig. S1*I*), the brassinosteroid deficiency of young *brx* roots (Fig. S1*J*), and the observation that brassinosteroid application restores *PIN3* expression in *brx* (16) support this idea.

BRX has been described as a rate-limiting component of auxin response; however, auxin perception is still functional in *brx* mutants (16, 21). Our finding that *BRX* serves to enhance *PIN* expression and thus possibly auxin perception above generic levels resolves this paradox. A straightforward explanation for a positive role of *BRX* in auxin perception would be a direct stimulation of auxin-responsive transcription, for example, through interaction with ARFs, a prediction that also emerged from network modeling of auxin–brassinosteroid interaction. Because of the observed genetic interaction between *brx* and *mp*, we tested this idea by in vitro protein interaction as well as by yeast two-hybrid assays. With both methods, we indeed found a strong interaction between BRX and the MP C terminus (Fig. 4 *A* and *B*; Fig. S1*K*); however, the interaction was outside of the conserved region where MP interacts with AUX/IAA proteins such as SHY2 (30) (Fig. 4 *C–E*). Given that BRX possesses transcription activation potential (13), this could mean that BRX amplifies MP activity or competitively shields MP from interaction with AUX/IAAs. This would also be consistent with described *BRX* gain-of-function phenotypes that resemble enhanced auxin perception phenotypes (14), including longer roots (12). In the root meristem context, BRX and SHY2 thus might compete to regulate ARFs. Because both genes are themselves feedback-regulated by the auxin pathway, their dynamic equilibrium would thus determine ARF activity. However, such an equilibrium could be maintained only if down-regulation of *BRX* by SHY2 would negatively feedback on *SHY2* expression. This appears to be the case, as *SHY2* is among the few

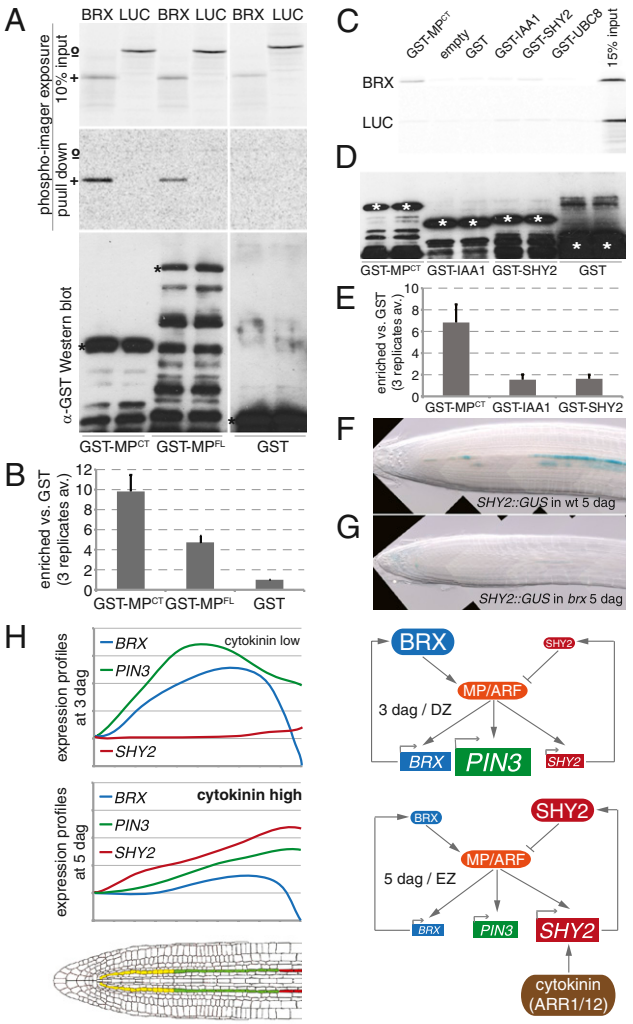

Fig. 4. Interaction of BRX and MP. (*A*) In vitro interaction assay between GST and GST-fused full-length (FL) or C-terminal (CT; amino acids 648–902) MP protein (asterisks) and radio-labeled BRX (plus sign) or luciferase (LUC) protein (open circle). (*B*) Quantification of BRX pull-down across three replicate experiments as described in *A*. (*C*) In vitro interaction assays including GST fusions of AUX/IAA (IAA1, SHY2) and additional control proteins (UBC8). (*D*) Western blot quantification of C-terminal MP and AUX/IAA fusion proteins used in assays. (*E*) Quantification of BRX pull-down across three replicate experiments as described in *C*. (*F* and *G*) *SHY2::GUS* expression in wild-type (wt) (*F*) and *brx* (*G*) at 5 dag. (*H*) Model of spatio-temporal equilibrium between *BRX*, *SHY2*, and *PIN3* expression profiles and the concomitant shifts in the proposed regulatory network. DZ: division zone; EZ: elongation zone.

auxin pathway genes that are no longer auxin-responsive and under-expressed in *brx* at 3 dag (16), a result that we corroborated by analysis of the *SHY2::GUS* reporter gene in *brx* mutants (Fig. 4 *F* and *G*). The equilibrium could eventually be shifted by an additional cue, i.e., the supplementary induction of *SHY2* expression by the cytokinin pathway in the transition zone, which would enable SHY2 to prevail in ARF regulation and result in a shutdown of *BRX* expression (Fig. 4*H*).

Collectively, our data suggest a spatio-temporal sequence of events that steers the transition of protophloem cells from proliferation to differentiation and simultaneously impinges on root meristem growth. This sequence involves a shift from preferential *BRX* expression toward preferential *SHY2* expression, which is intimately linked to the spatial component of a changing position along the auxin gradient. Through the downstream effect on *PIN3* expression, this regulatory module determines the time frame for meristem growth and consequently the subsequent root growth rate. At later stages, equally dynamic *BRX* expression patterns can be observed in other root tissue layers as well as in processes where *brx* displays quantitative phenotypes (14, 15). Thus, the described regulatory module might serve to regulate the transition toward differentiation in various contexts, which would also explain the remarkable conservation of *BRX* and related genes across the flowering plants (12).

Materials and Methods

Plant Materials. The Arabidopsis *brx-2* null allele used throughout this study [except in Fig. 1*M*, which used the brx^{C} null mutant (13)] has been described (31), as have the *shy2-D*, *shy2-31* (9), and mp^{S319} (3) mutants. The *35S::BRX:GFP* (21), *PIN3::PIN3:GFP* (7), *PIN1::PIN1:GFP* (7), *BRX::GUS* (21), *SHY2::GUS* (9), and *SHY2::YFP* transgenes were introduced into wild-type (Col-0) or mutant backgrounds through crossing or transformation. Plant tissue culture and transgenesis were performed as described (15, 21).

Microscopy. For confocal microscopy, roots of seedlings grown on solid media were placed in liquid media, including any treatments (except those in Fig. 3 *J* and *K*, which were placed on solid media) before analysis using a Leica SP2 AOBS confocal laser scanning microscope (CLSM). All images were taken with an offset of less than 5%. β-Glucuronidase (GUS) staining and light microscopy were performed according to standard procedures using a Leica DM5000B compound microscope. All images shown or analyzed within one experiment were taken at identical settings for all genotypes investigated. For analysis of embryo phenotypes, ovules were collected and fixed in chloral hydrate:glycerol:H_2O (8:3:1) solution. The modified pseudo-Schiff (mPS)-propidium iodide (PI) staining method for visualization of the cell walls in developing protophloem has been described (2).

Molecular Biology. Molecular biology procedures such as cloning, genotyping, and qPCR followed standard protocols as described (14, 15). All qPCR plots represent averages from three or more independent replicate experiments. The following oligonucleotides were used for qPCR amplification: CCA GGA TCT GTC CCG CAT CAC TTT and CTG TTC TGC TCC CAC CAT GTC TTT for *BRX* coding sequence; GGC CTG TCA AAT GTA TCG TGA C and GAG AAG TCG GGT TAT TGG GTG A for *BRX* promoter (ChIP experiment); CCA TGT CGT GTG TTT TGT GAC A and GGT GAC TTT CCT CCA AGT TTA TG for *BRX* 3′ UTR (ChIP experiment); GAC CAG CTC TTC CAT CGA GAA and CAA ACG AGG GCT GGA ACA AG for *ACTIN2*; GGA GAC TTA AGT AGG AGC TCA GCA and CCA AAA GAG GAA ACA CGA ATG for *PIN1*; TCT TTG ATT AGG TTC GGG TAA CTC and GCT CAT GTG AAA CTG GAA CAA G for *PIN3*; ACA ACG CCG TTA AAT ATG GA and AGA CCC CAT TTT ATT CAG CC for *PIN4*; and CCA AGA TTA GTG GAA CGC AAC and GAA AAG GGT TTT TGG ATC CTC for *PIN7*.

For band shift assays, an N-terminal MP fragment encompassing amino acids 1–432 and including the DNA-binding domain was expressed with a His-tag fused to its N terminus in an *Escherichia coli* expression system. Control reactions contained either a control protein purification from bacteria harboring an empty expression vector or an unrelated, purified prokaryotic protein with the same amino-terminal His-tag. Increasing amounts (10×, 50×, 100×) of specific or unspecific unlabeled probe DNA were added as competitor. The unspecific unlabeled DNA lacked a consensus auxin response element. Chromatin immunoprecipitation assays were performed as described (3). For in vitro protein interaction assays, GST fusion proteins were purified according to standard protocols. Pull-down assays with radio-labeled BRX or LUC protein derived from in vitro transcription/translation wheat germ reactions (Invitrogen) were performed as described (32).

Brassinosteroid Quantification. Major active brassinosteroids in 4-d-old wild-type and *brx* seedlings were determined as described (14).

Quantification of Expression Profiles. All measurements were performed with ImageJ software (version 1.43r). Images of GUS-stained *BRX::GUS* or *SHY2::GUS* root meristems were acquired at different positions along the root tip to ensure sufficient resolution. Different images from the same root and focal plane were aligned using blending to overlap the images and record the relative coordinates of each picture. Care was taken to analyze only images where the protophloem could be followed in the focal plane from the start of the division zone into the elongation zone. A segmented line was used as the region of interest (ROI) along the protophloem starting from the quiescent center and ending in the first cell of the protophloem

elongation zone. The ROI line traversed the phloem at the center of the cells. Use of other types of ROIs confirmed the segmented line as the best indicator for the expression pattern. Images were converted to an eight-bit format, the gray scale range was inverted, and the dimension scale of the image was set in microns according to the microscope metadata. A plot profile of the gray values was recorded for each ROI, providing a measurement of GUS intensity where higher values point to darker staining and higher expression.

Measurements of CSLM image stacks from *35S::BRX:GFP* to determine plasma membrane abundance were performed as follows. First, all stacks from the same root were aligned using an internal slice with a clear cell profile. Slices were superimposed on one another by blending to record the relative coordinates of each image. Stacks were then merged using the Stack Inserter plug-in of ImageJ. In the final stack, the protophloem was identified by mPS-PI staining (2), because differentiating protophloem cell walls are brighter than those of surrounding tissues. The PI channel was also used for placing the ROI at the basal membrane of each phloem cell. An appropriately sized rectangular ROI was defined to encompass the basal membrane of cells, where BRX-GFP protein is localized at the poles. For measurements within each stack, the same ROI was maintained and ROIs among different stacks were chosen in adjacent areas for comparison. For each ROI, mean intensity was recorded across all of the slices in a stack. Only cells with GFP expression above detection levels were considered. Data were filtered using R version 2.10.0 to retain only the measurements on the slices traversing each cell identified by a particular ROI. Data were thus averaged across slices.

For measurements of PIN3-GFP and PIN1-GFP expression across the root meristem, a segmented line with a width equal to 100 pixels was chosen to include both protophloem poles. Plot profiles were recorded over a slice range that started from the first slice traversing the first phloem to the last slice crossing the second phloem. Intensity measures were normalized in percentages according to the maximum intensity per each slice. For each point along the segmented line, the mean across all of the slices considered in the stack was taken.

In both GUS staining and GFP expression measurements, data were normalized separately for each phloem. Intensities were scaled in percentages according to the maximum intensity across the phloem. Position in microns for pixels and ROI centers were scaled in percentages with 0% referring to the start of the division zone and 100% to the last point of the line. For presentation, measurements where scaled to start each curve at the same value of 100% because the overall trends of the curves and not the absolute intensity values were compared. For final quantification, signals were binned in 5% or 10% increments, depending on the continuity of the type of marker scored. For example, GUS staining reporting transcription levels was continuously spread throughout cells and could be binned in 1% increments across all samples analyzed to give robust quantification. By contrast, BRX-GFP signal had to be binned in 10% increments to attract sufficient signal across the samples because of the discontinuity introduced by the polar plasma membrane localization of BRX-GFP when analyzed in a single cell file.

ACKNOWLEDGMENTS. We thank Drs. S. Sabatini (University "La Sapienza", Rome Italy), G. Juergens (Tuebingen Plant Science Center, Germany), D. Weijers (Wageningen University, The Netherlands), and Y. Helariutta (University of Helsinki, Finland) for providing materials; D. Tarkowska and M. Strnad for brassinosteroid measurements; and J.-C. Palauqui for discussions. We also thank A.-M. Amiguet-Vercher for technical support. This work was supported by Swiss National Science Foundation Grant 31003A_129783, by the BRAVISSIMO Marie-Curie Initial Training Network (E.S.), and by a European Molecular Biology Organization long-term postdoctoral fellowship (to L.R.).

1. Dolan L, et al. (1993) Cellular organisation of the Arabidopsis thaliana root. *Development* 119:71–84.
2. Truernit E, et al. (2008) High-resolution whole-mount imaging of three-dimensional tissue organization and gene expression enables the study of phloem development and structure in Arabidopsis. *Plant Cell* 20:1494–1503.
3. Schlereth A, et al. (2010) MONOPTEROS controls embryonic root initiation by regulating a mobile transcription factor. *Nature* 464:913–916.
4. Sabatini S, et al. (1999) An auxin-dependent distal organizer of pattern and polarity in the Arabidopsis root. *Cell* 99:463–472.
5. Benjamins R, Scheres B (2008) Auxin: The looping star in plant development. *Annu Rev Plant Biol* 59:443–465.
6. Grieneisen VA, Xu J, Marée AF, Hogeweg P, Scheres B (2007) Auxin transport is sufficient to generate a maximum and gradient guiding root growth. *Nature* 449: 1008–1013.
7. Benková E, et al. (2003) Local, efflux-dependent auxin gradients as a common module for plant organ formation. *Cell* 115:591–602.
8. Dello Ioio R, et al. (2007) Cytokinins determine Arabidopsis root-meristem size by controlling cell differentiation. *Curr Biol* 17:678–682.
9. Dello Ioio R, et al. (2008) A genetic framework for the control of cell division and differentiation in the root meristem. *Science* 322:1380–1384.
10. Moubayidin L, Di Mambro R, Sabatini S (2009) Cytokinin-auxin crosstalk. *Trends Plant Sci* 14:557–562.
11. Weijers D, et al. (2005) Developmental specificity of auxin response by pairs of ARF and Aux/IAA transcriptional regulators. *EMBO J* 24:1874–1885.
12. Beuchat J, et al. (2010) A hyperactive quantitative trait locus allele of Arabidopsis BRX contributes to natural variation in root growth vigor. *Proc Natl Acad Sci USA* 107: 8475–8480.
13. Mouchel CF, Briggs GC, Hardtke CS (2004) Natural genetic variation in Arabidopsis identifies BREVIS RADIX, a novel regulator of cell proliferation and elongation in the root. *Genes Dev* 18:700–714.
14. Beuchat J, et al. (2010) BRX promotes Arabidopsis shoot growth. *New Phytol* 188: 23–29.
15. Sibout R, Plantegenet S, Hardtke CS (2008) Flowering as a condition for xylem expansion in Arabidopsis hypocotyl and root. *Curr Biol* 18:458–463.
16. Mouchel CF, Osmont KS, Hardtke CS (2006) BRX mediates feedback between brassinosteroid levels and auxin signalling in root growth. *Nature* 443:458–461.
17. Bao F, et al. (2004) Brassinosteroids interact with auxin to promote lateral root development in Arabidopsis. *Plant Physiol* 134:1624–1631.
18. Hardtke CS (2007) Transcriptional auxin-brassinosteroid crosstalk: Who's talking? *Bioessays* 29:1115–1123.
19. Li L, Xu J, Xu ZH, Xue HW (2005) Brassinosteroids stimulate plant tropisms through modulation of polar auxin transport in Brassica and Arabidopsis. *Plant Cell* 17: 2738–2753.
20. Nemhauser JL, Mockler TC, Chory J (2004) Interdependency of brassinosteroid and auxin signaling in Arabidopsis. *PLoS Biol* 2:E258.
21. Scacchi E, et al. (2009) Dynamic, auxin-responsive plasma membrane-to-nucleus movement of Arabidopsis BRX. *Development* 136:2059–2067.
22. Moubayidin L, et al. (2010) The rate of cell differentiation controls the Arabidopsis root meristem growth phase. *Curr Biol* 20:1138–1143.
23. Bonke M, Thitamadee S, Mähönen AP, Hauser MT, Helariutta Y (2003) APL regulates vascular tissue identity in Arabidopsis. *Nature* 426:181–186.
24. Bauby H, Divol F, Truernit E, Grandjean O, Palauqui JC (2007) Protophloem differentiation in early Arabidopsis thaliana development. *Plant Cell Physiol* 48:97–109.
25. Hardtke CS, Berleth T (1998) The Arabidopsis gene MONOPTEROS encodes a transcription factor mediating embryo axis formation and vascular development. *EMBO J* 17: 1405–1411.
26. Donner TJ, Sherr I, Scarpella E (2009) Regulation of preprocambial cell state acquisition by auxin signaling in Arabidopsis leaves. *Development* 136:3235–3246.
27. Birnbaum K, et al. (2003) A gene expression map of the Arabidopsis root. *Science* 302: 1956–1960.
28. Vieten A, et al. (2005) Functional redundancy of PIN proteins is accompanied by auxin-dependent cross-regulation of PIN expression. *Development* 132:4521–4531.
29. Symons GM, Ross JJ, Jager CE, Reid JB (2008) Brassinosteroid transport. *J Exp Bot* 59: 17–24.
30. Guilfoyle TJ, Hagen G (2007) Auxin response factors. *Curr Opin Plant Biol* 10:453–460.
31. Rodrigues A, et al. (2009) The short-rooted phenotype of the brevis radix mutant partly reflects root abscisic acid hypersensitivity. *Plant Physiol* 149:1917–1928.
32. Hardtke CS, et al. (2000) HY5 stability and activity in Arabidopsis is regulated by phosphorylation in its COP1 binding domain. *EMBO J* 19:4997–5006.